EUROFUSION WPJET1-CP(16) 15069

JR Martin-Solis et al.

Current profile shape effects on the formation and termination of runaway beams in tokamak disruptions and implications for ITER

Preprint of Paper to be submitted for publication in
Proceedings of 26th IAEA Fusion Energy Conference

This work has been carried out within the framework of the EUROfusion Consortium and has received funding from the Euratom research and training programme 2014-2018 under grant agreement No 633053. The views and opinions expressed herein do not necessarily reflect those of the European Commission.

Current profile shape effects on the formation and termination of runaway beams in tokamak disruptions and implications for ITER

J.R. Martín Solís[1], A. Loarte[2], M. Lehnen[2], P. Abreu[3,4], I. Lupelli[4], C. Reux[5], V. Riccardo[4], G. Szepesi[4] and JET Contributors[*]

EUROfusion Consortium, JET, Culham Science Centre, Abingdon, OX14 3DB, UK

[1] Universidad Carlos III de Madrid, Avenida de la Universidad 30,28911-Madrid, Spain
[2] ITER Organization, Route de Vinon-sur-Verdon, CS 90046, 13067 St Paul Lez Durance Cedex,France
[3] Instituto de Plasmas e Fusão Nuclear, Instituto Superior Técnico, Univ. de Lisboa, Portugal
[4] Culham Centre for Fusion Energy, Culham Science Centre, Abingdon, OX14 3DB, UK
[5] CEA, IRFM, F-13108 Saint-Paul-lez-Durance, France

e-mail contact of main author: solis@fis.uc3m.es

Abstract. A one dimensional (1-D) model is used to evaluate effects associated with the evolution of the ohmic plasma and runaway (RE) beam current profiles during the current quench (CQ) and termination phases of tokamak disruptions. The model predictions are in agreement with the estimated values of the plasma internal inductance, l_{int}, for JET low elongation limiter discharges with 2 MA plasma current in which disruptions were triggered to form RE current plateau plasmas. It is found that the final RE current density profile is more peaked that the current profile before the disruptive event, the peaking of the current profile decreasing when the RE current increases. In order to investigate these effects in ITER, an integrated analysis of the RE beam formation and termination during ITER disruptions has been carried out using the 1-D model of the disruption and including: a) the expected RE generation mechanisms, and b) corrections to the RE electron dynamics to account for the collisions of the runaway electrons with the partially stripped impurity ions. Mitigated disruptions by Ar or Ne injection injected before the current quench have been considered and the CQ times have been kept within the range compatible with acceptable forces on the ITER vessel and in-vessel components. The lowest RE production is found for the shortest CQ times, particularly for the case of Ne, due to the collisions of the REs with the impurity ions. For the case of long CQ times, runaway beams up to ~10 MA can be generated, and the energy deposited by the REs on the PFCs during the termination phase can increase to a few hundreds of MJs, mainly due to the avalanche generation of REs during the termination phase. The peaking of the RE beam is indeed found to decrease with the RE current fraction and the examination of the plasma trajectories in l_{int} - q_a space suggests that the beam crosses the high-l_{int} empirical stability boundary before the expected time in ITER for the vertical instability growth (~100 ms), although, by that time, the beam is essentially formed. The RE current profile peaking also enhances significantly the role played by the RE avalanche during current termination, increasing the energy conversion efficiency in comparison with zero-dimensional calculations. Mixed impurity (Ar or Ne) plus deuterium injection is found to be effective in controlling the formation of the RE current during the current quench as well as the energy deposited on the REs during current termination.

1. Introduction

Runaway electrons (REs) generated during disruptions are usually found to deposit their energy in very short pulses and on localized areas of the plasma facing components (PFCs). In ITER, there is serious concern about the potential that large amounts of MeV REs generated during the disruption current quench (CQ) have for erosion / melting of the PFCs. Although zero-dimensional (0-D) modeling has shown to provide a rather complete physics picture of the CQ and termination phases of the disruption [1,2], there is evidence indicating that current profile shape effects could be important [3,4,5]. Hence, self-consistent modeling of the plasma and RE current density profiles during disruptions has predicted a substantial peaking of the current profile during the generation of the RE current [3,5] which indeed has been supported by JET observations [4]. Here, a one-dimensional model (1-D) is used to evaluate effects associated with the evolution of the plasma and RE current profiles during the

[*] **See the author list of "Overview of the JET results in support to ITER" by X. Litaudon et al.** to be published in Nuclear Fusion Special issue: overview and summary reports from the 26th Fusion Energy Conference (Kyoto, Japan, 17-22 October 2016)

disruption. The model predictions are found to be in agreement with measurements of the plasma internal inductance for 2 MA JET disruptions with RE current plateau formation (Sec.2). The resulting runaway plasma is more peaked in the plasma center than the pre-disruption plasma current and the peaking is observed to decrease when the RE current increases. Extrapolation to ITER disruptions is addressed in Sec.3, where an integrated modeling of runaway generation and termination using the 1-D model is presented for selected ITER scenarios. Mitigated disruptions with Ar, Ne as well as mixed Ar+D and Ne+D injection are considered. The effect of the expected RE generation mechanisms in ITER (avalanche and RE primary seeds) is included, together with a proper treatment of the RE dynamics in plasmas with high impurity content. The conclusions are summarized in Sec.4.

2. Current profile shape effects during RE plateau formation in JET disruptions

Fig.1 (left) shows 2 MA JET disruptions with runaway current plateau formation ~1 MA. The current profile peaking is quantified by the plasma internal inductance [4], l_{int}, shown in the right figure, which is estimated by means of plasma equilibrium reconstruction with EFIT: l_{int} is inferred from the Shafranov Λ, $\Lambda = \beta_p + l_{int}/2$, where β_p is the poloidal beta of the plasma provided that the relativistic beam pressure is taken into account to calculate the effective β_p of the runaway plasma [4]:

$$\beta_p^r = \frac{(\gamma \times v/c) I_{A0} I_r}{I_p^2}, \qquad (1)$$

where v/c is the ratio of the runaway electron velocity to the speed of light, $\gamma = (1 - v^2/c^2)^{-1/2}$ is the electron relativistic gamma factor and $I_{A0} \approx 17$ kA (a monoenergetic beam is assumed for simplicity). The full lines in the right figure shows the time evolution of 2Λ (l_{int} if $\beta_p = 0$ is assumed). The strong increase in l_{int} at ~10.433 *s* is a distinctive feature of the replacement of the plasma current by the runaway current.

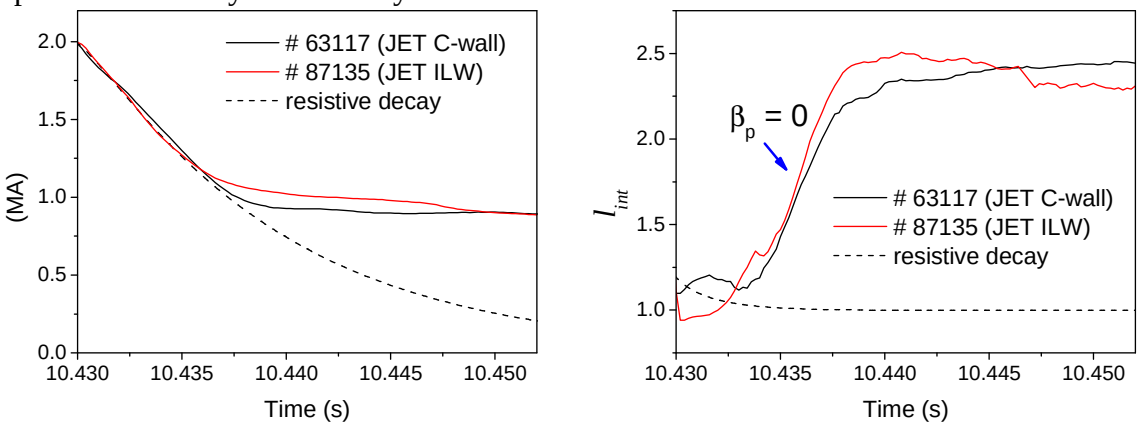

FIG.1 JET disruptions showing the formation of ~1MA RE current (black: JET carbon wall; red: JET ITER-LikeWall (ILW)): Left: Measured plasma current (full line), and simulation carried out assuming pure resistive decay (dashed line); Right: l_{int} evolution estimated from the Shafranov Λ ($\beta_p = 0$) (full line) and calculated for the pure resistive decay case (dashed line).

The dashed lines correspond to simulations of the current evolution carried out by means of a one-dimensional (1-D) model in cylindrical geometry, that takes into account the evolution of the plasma current density profile during the disruption current quench [5], assuming a pure resistive current decay (no runaways generated) and reproducing the initial CQ rate,

$$\mu_0 \frac{\partial j_p}{\partial t} = \frac{1}{r}\frac{\partial}{\partial r}\left[r \frac{\partial E_\parallel}{\partial r} \right] = \frac{1}{r}\frac{\partial}{\partial r}\left[r \frac{\partial \eta j_p}{\partial r} \right], \qquad (2)$$

where η is the plasma resistivity and j_p is the plasma current density. In this case, no peaking (l_{int} increase) is observed during the current quench.

Fig.2 shows the measured l_{int} of the RE plasma for a set of 2 MA purposely triggered disruptions in JET showing the formation of a plateau runaway current in a range ~ 0.7 - 1.3 MA. The discharges are all in limiter configuration. The estimates of l_{int} assuming $\beta_p = 0$ and including corrections due the poloidal β of the runaway plasmas (for a typical energy for disruption generated REs in JET, E ~ 8 MeV) are compared and the estimated internal plasma inductance at the start of the CQ, l_{int}^{0}, is also shown for illustration. In agreement with theoretical expectations, not only the runaway current density profile is more peaked than the initial plasma current, but the peaking decreases when the runaway current increases [5]. 1-D simulations of the current decay and RE generation have been carried out including in Eq.(2) the replacement of the plasma current by the runaway current, $E_{\|} = \eta\, j_{OH} = \eta(j_p - j_r)$ (with $j_{p,r}$: plasma and runaway current densities, respectively),

$$\mu_0 \frac{\partial j_p}{\partial t} = \frac{1}{r}\frac{\partial}{\partial r}\left[r \frac{\partial E_{\|}}{\partial r} \right] = \frac{1}{r}\frac{\partial}{\partial r}\left[r \frac{\partial \eta (j_p - j_r)}{\partial r} \right], \tag{3}$$

and an equation describing the runaway generation, which includes the primary (Dreicer) and secondary generation of runaway electrons,

$$\frac{\partial n_r}{\partial t} = n_e \nu_{coll} \lambda + \frac{n_r}{\tau_s} \tag{4}$$

where ν_{coll} is the collision frequency, λ is the Dreicer birth rate [6] and τ_s represents the typical avalanching time [7]. The runaway current is estimated by assuming that all runaways travel at the speed of light ($j_r = e c n_r$). Although the lack of knowledge of the plasma parameters during the disruption prevents an accurate analysis, the 1-D simulations (red line) are consistent with the observed behavior of l_{int}. The modeling assumes the avalanche amplification of an initial runaway seed and the black lines in the figure correspond to two set of simulations obtained increasing the runaway seed current, I_{seed}, but keeping constant the seed profile shape (l_{int}^{seed} = 1.2 and 1.9). The resulting l_{int} increases with l_{int}^{seed} and decreases when I_r increases but the decay is too slow to explain the observations. However, if the runaway seed is assumed to be due to the Dreicer mechanism (red line), the seed profile shape is not constant but l_{int}^{seed} decreases when the Dreicer seed increases which eventually leads to a faster decay of l_{int} in consistency with the measurements.

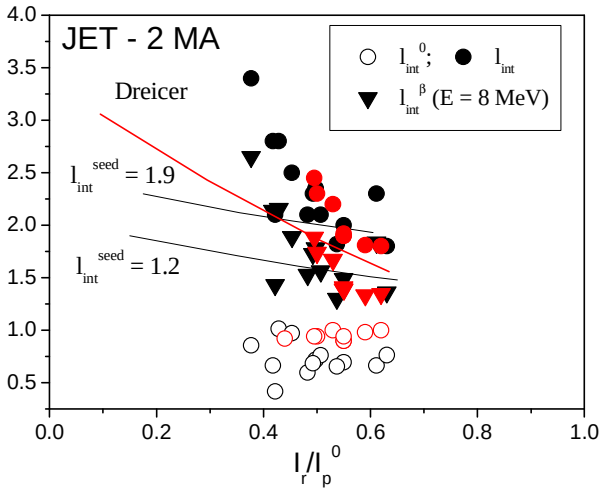

FIG.2 Estimated l_{int} of the RE plasma for 2 MA JET disruptions (black: JET C wall; red: JET ILW) vs. RE current fraction: assuming $\beta_p = 0$ (full circles) and corrections by β_p^r (E = 8 MeV) (triangles). The estimated internal plasma inductance at the start of the CQ, l_{int}^{0}, is also shown (open circles). Red line: 1-D simulations carried out using the Dreicer seed; Black lines: 1-D simulations obtained increasing I_{seed} and assuming constant l_{int}^{seed} (1.2 and 1.9).

These observations might have important implications for ITER: (1) due to the increase of l_{int}, for the same RE current magnitude, the magnetic energy of the RE plasma could be substantially larger; (2) as the current peaking of the runaway beam (l_{int}) depends on the magnitude of the runaway current (I_r), the runaway plasma magnetic energy does not scale linearly with I_r^2, which can counteract the effect described in (1): (3) the post-CQ plasma current profile might be MHD unstable as plasmas with peaked current profiles can be prone to the tearing-mode instability. The consequences of the current profile peaking for the stability of the RE beam are illustrated in Fig.3 which shows l_{int} vs. the edge q for the RE plasmas of Fig.2 together with the high-l_{int} empirical stability boundary for JET limiter disruptions (full line). The calculated l_{int} tends to be in a range corresponding to MHD unstable regions in the l_{int}-q_a diagram. Indeed, these RE plasmas are observed to become unstable and finally lost, although the processes leading to their termination are not well understood and difficult to identify from the observations.

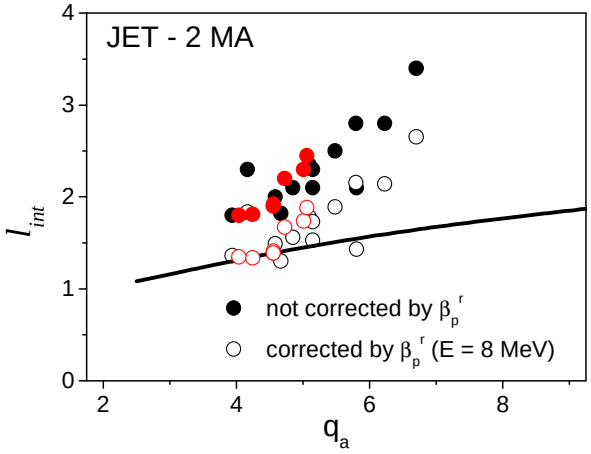

FIG.3 l_{int} vs. edge q (black: JET C wall; red: JET ILW) for the RE plasmas of Fig.2 (full circles: β_p^r = 0; open circles: corrected by β_p^r for E = 8 MeV). The high-l_{int} empirical stability boundary (full line) is indicated.

3. Modeling of runaway beam formation and termination in ITER disruptions

The RE beam formation and termination in ITER disruptions has been analysed using the 1-D model described above [Eqs.(3) and (4)] for selected scenarios ranging from 5 MA to 15 MA DT H-mode and L-mode plasmas. We will focus on the results for H-mode plasmas as they have the largest seeds due to their higher temperatures and fusion production. Mitigated disruptions by Ar and Ne injection are considered. For a given impurity density, n_z, the temperature, T_e, is determined using the power balance relation, $\eta j_{OH}^2 = n_{ef}\, n_z\, L_{imp}$, where $n_{ef} = n_H + \langle Z \rangle\, n_z$ is the free electron density (n_H is the total hydrogen, DT, density), $\langle Z \rangle$ is the averaged impurity charge and L_{imp} the radiative cooling rate (atomic data taken from the ADAS database). The resulting exponential current decay rate is chosen to be consistent with acceptable forces on the ITER vessel and in-vessel components (τ_{res} ~ 22 - 66 ms for 15 MA disruptions) [8]. It should be noted that evaluating τ_{res} by applying a 0-D model of the current decay [2,8] ($\tau_{res} \approx La^2/2R_0\eta$) results in a substantial overestimate of the amount of the impurities required to obtain a given τ_{res} in comparison with 1-D CQ simulations. This is illustrated Fig.4 which shows, for a 15 MA disruption and $n_H = 10^{20}$ m^{-3}, Ar (circles) and Ne (triangles), the 0-D (black symbols) and 1-D (open symbols) estimates of the number of injected atoms (in kPa·m^3) assuming 100% assimilation efficiency vs. τ_{res}. The largest amount of impurities is found for the shortest τ_{res} which for Ar requires ~0.1 kPa·m^3 (T_e ~ 4 eV) while, for Ne, with a much lower radiation rate at low T_e, it requires ~6 kPa·m^3 (T_e ~ 3 eV).

The generation of the RE current is assumed to take place by the formation of a runaway seed at the start of the CQ followed by the avalanche seed amplification. The primary RE seeds are estimated following Ref.[2] and include the Dreicer mechanism, the hot-tail RE generation,

the tritium decay seed, and the Compton source. Corrections to the runaway dynamics and generation are considered to account for the collisions of the REs with the impurity ions, including the collisions with the free and bound electrons as well as the penetration of the REs through the electronic shell of the partially stripped impurities [2].

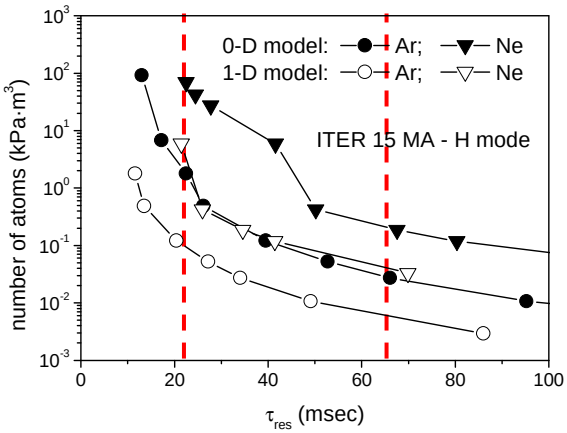

FIG.4 Comparison between the 0-D (black symbols) and 1-D (open symbols) evaluations of the number of injected atoms (in kPa·m^3) assuming 100% assimilation efficiency vs. τ_{res} for Ar (circles) and Ne (triangles) (15 MA current, $n_H = 10^{20}$ m^{-3}). The vertical red dashed lines indicate the range of τ_{res} values leading to acceptable forces onto the vessel and in-vessel components in ITER.

No RE losses are considered during the CQ phase. The termination phase is modelled including a loss term for the RE current in Eq.(4), - n_r/τ_{diff}, with characteristic timescale τ_{diff} (τ_{diff} = 0.1 - 10 ms [1]) at the expected time in ITER for the vertical instability growth (~ 100 ms) [9]. The example of Fig.5 shows a 15 MA H-mode disruption with Ar injection and τ_{res} = 34 ms. At 100 ms, the runaway current (left) is ~9 MA and the RE beam kinetic energy (right) ~21 MJ. Then, the termination phase starts (τ_{diff} = 5 ms) and the plasma current and the REs are lost. The loss of the current gives rise to an induced electric field and an ohmic current, and magnetic energy is converted into RE kinetic energy, the total energy deposited by the REs $W_{run} = W_{run}^0 + \Delta W_{run}$, where W_{run}^0 is the runaway kinetic energy at the start of the termination phase (~21 MJ) and ΔW_{run} the magnetic energy converted into RE kinetic energy during current termination, $\Delta W_{run} \sim$ 172 MJ, so that $W_{run} \sim$ 193 MJ.

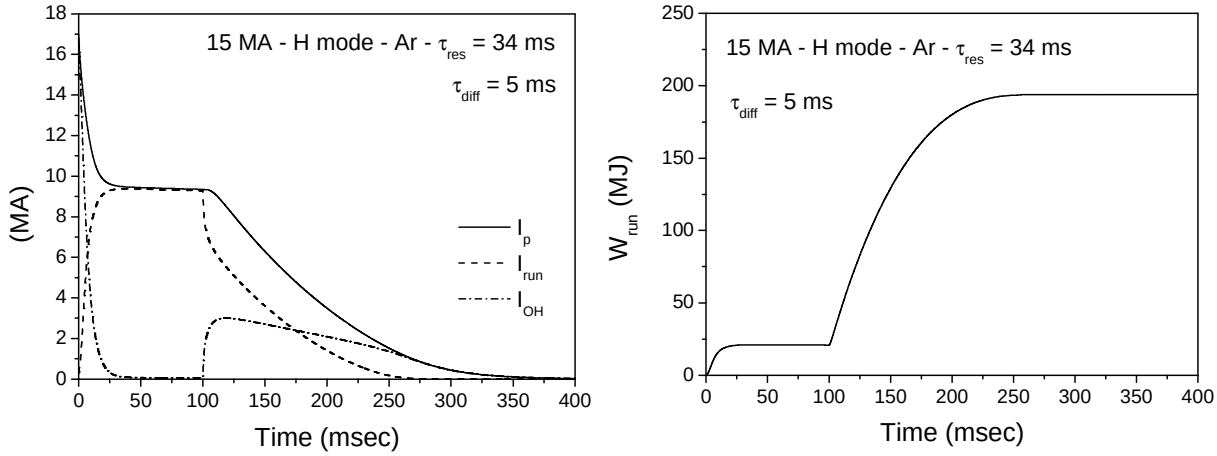

FIG5 For a 15 MA H-mode disruption with Ar injection, τ_{res} = 34 ms: Left: Time evolution of the plasma current (I_p) , runaway current (I_{run}) and ohmic current (I_{OH}) during the CQ and termination phase of the disruption (τ_{diff} = 5 ms); Right: Time evolution of runaway kinetic energy gain.

The predicted RE current at 100 ms is plotted in Fig.6 (left) for 15 MA H-mode disruptions with Ar vs. τ_{res}. The predictions for the different runaway primary seeds are compared (in case that a few or all of them are acting together, the final result will be dominated by the largest one). The collisions of the REs with impurity ions can play an important role, particularly for Ne injection because of the large amount required due its small radiation efficiency at low T_e, leading to low runaway production and energy conversion during current

termination for the shortest CQs (~22 ms). For the longest CQs, significant RE currents can be found and several primary runaway mechanisms can make a significant contribution. Dreicer generation is found to be always negligible. A strong dependence is also found on the pre-disruption plasma current and, at 5 MA, the predicted RE current is less than 2 MA.

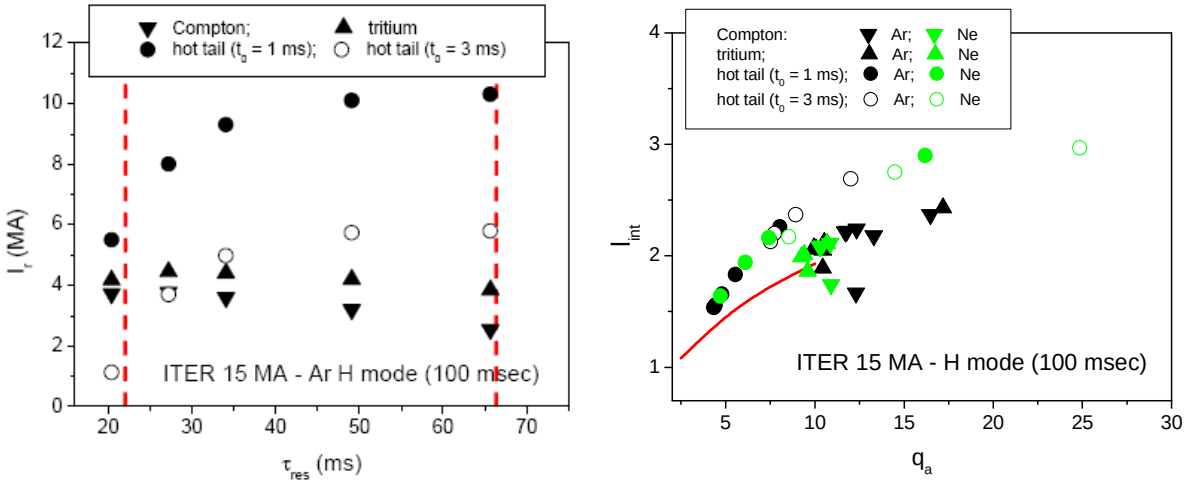

FIG.6 Left: Predicted RE current at 100 ms vs. τ_{res} for 15 MA H-mode disruptions with Ar injection (t_0: characteristic thermal quench duration). The vertical red lines show the range of τ_{res} values for acceptable mechanical loads in ITER; Right: Plasma parameters at 100 ms in l_{int}-q_a space for 15 MA ITER disruptions, Ar and Ne injection, and τ_{res} = 22−66 ms. The high-l_{int} empirical stability boundary (red line) is also indicated.

The effects associated with the evolution of the plasma and RE current profiles during the CQ phase of 15 MA H-mode disruptions with Ar and Ne injection and τ_{res} ~ 22 - 66 ms are illustrated in Fig.6 (right). The figure shows the plasma parameters at 100 ms in l_{int} - q_a space (the red line corresponds to the high-l_{int} empirical boundary) and it illustrates the peaking of the RE current density profile in comparison with the initial (at the start of the CQ) plasma current (flattish profile, l_{int}^{0} ~0.7). The peaking is larger (higher l_{int}) for the case of the hot-tail seeds due to the significant peaking of the hot-tail RE seed profiles (high l_{int}^{seed}) while the Compton and tritium RE seed profiles are usually quite flat (low l_{int}^{seed}). The increase of l_{int} with q_a is associated with the decrease of the l_{int} when I_r increases discussed in Sec.2. The figure also suggests that, in most of the cases, the runaway beam may become MHD unstable: the Compton and tritium seed cases typically cluster close (and above) to the high-l_{int} boundary, while the hot-tail seed cases, with a substantially larger l_{int}, can lie well above this boundary. Nevertheless, it should be noted that by the time (t_{stab}) at which the plasma crosses the stability boundary in l_{int} - q_a space, the RE beam is almost fully formed and its current and energy values do not significantly differ from those at 100 ms.

Fig.7 (left) shows the total energy deposited on PFCs by REs during the termination phase, W_{run}, vs. τ_{diff} for 15 MA disruptions with Ar injection, τ_{res} ~ 34 ms and three selected cases with different runaway seeds showing a significant RE formation during the current quench (Fig.6). The REs are assumed to be lost in a single event and τ_{diff} = 0.1 - 10 ms [1]. During fast terminations (small τ_{diff}), the conversion of magnetic into RE kinetic energy is negligible ($W_{run} \sim W_{run}^{0}$). However, when τ_{diff} increases, the avalanche RE generation plays an important role and the energy deposited by the runaways can be as large as a few hundreds of MJs (~ 10 × W_{run}^{0}) for the slowest terminations. The peaking of the RE current profile during the CQ phase increases the current density in the plasma center and, hence, the avalanche multiplication in the core plasma during current termination, leading to a larger energy conversion during the termination phase than in the 0-D modelling. The increase of l_{int} during

RE termination (right Fig.7) is the signature of a strong avalanche in the plasma center which increases with τ_{diff} and with the amount of RE current generated during the disruption CQ.

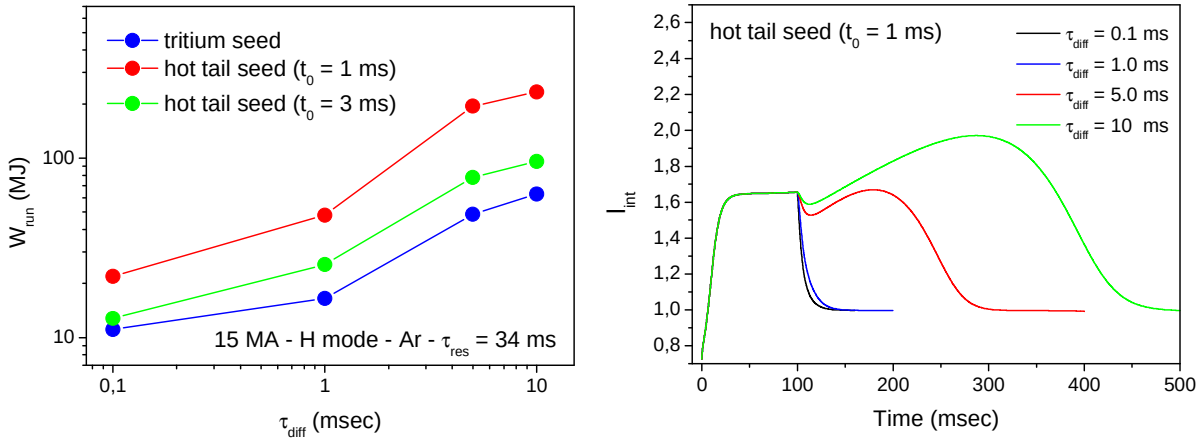

FIG.7 Left: W_{run}*, vs.* τ_{diff} *for selected scenarios of Fig.6; Right: Time evolution of* l_{int} *during RE beam formation and termination for the hot-tail seed (*t_0 *= 1ms) case and different values of* τ_{diff}*.*

Modelling of disruptions with mixed Ar+D and Ne+D injection has also been addressed (up to 14 kPa·m^3 D_2 injection). Deuterium does not radiate significantly so that mixed impurity (Ar or Ne) + D injection allows the achievement of disruption mitigation with similar CQ times to Ar and Ne injection alone but with increased plasma density due to presence of D. The injection of deuterium, increasing the plasma collisionality, has an effect on both the primary RE sources and the multiplication by avalanche of the runaway seed during the CQ phase. Fig.8 (left) shows the calculated RE beam magnetic energy (W_{mag}) at 100 ms for 15 MA Ar+D disruptions and τ_{res} ~ 22 - 66 ms as a function of the RE current. The maximum predicted W_{mag} decreases from ~300 MJ with Ar injection alone, to ~100 MJ for 3.5 kPa·m^3 D_2 injection, ~10 MJ for 7 kPa·m^3, to less than 1 MJ for ~14 kPa·m^3 D injection. Moreover, the injection of D also reduces the effects associated with the acceleration of the REs and the secondary RE generation on the conversion of magnetic into RE kinetic energy during RE termination. Hence, for 3.5 kPa·m^3 D injection, τ_{res} ~ 34 ms and hot-tail RE seed with t_0 as small as 0.1 ms, the total energy deposited onto PFCs by the REs during runaway termination decreases down to $W_{run} \sim 6 \times W_{run}^0$ (~80 MJ) (Fig.8 (right)). For Ar+7 kPa·m^3 D injection the total RE electron energy deposited onto PFCs is further decreased to only $W_{run} \sim 2 \times W_{run}^0$ (~7 MJ) and for ~14 kPa·m^3, D injection fully prevents the conversion of magnetic into runaway energy during disruption termination and the RE energy loads are less than 1 MJ.

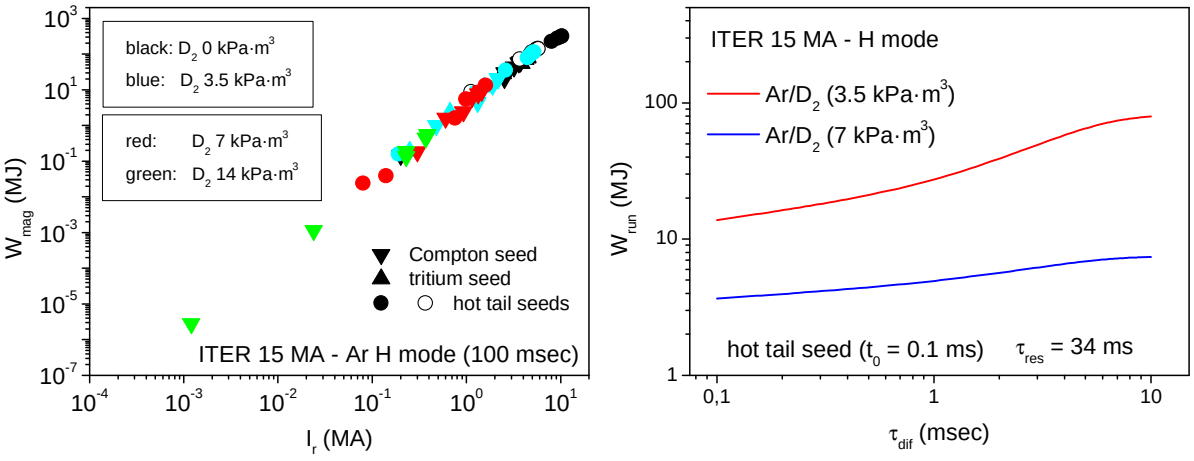

FIG.8 For 15 MA H-mode disruptions and Ar+D injection: Left: Magnetic energy of the RE beam at 100 ms vs. I_r*; Right:* W_{run} vs. τ_{diff} *for 3.5 kPa·m*^{3} *(red) and 7 kPa·m*^{3} *(blue) D injection.*

4. Conclusions

Current profile shape effects have been analyzed for 2 MA JET disruptions with RE current plateau formation. Measurements of l_{int} indicate that the RE plasma is more peaked in the plasma center than the initial plasma current density profile, the peaking decreasing when the runaway current increases in agreement with the theoretical expectations. The dependence of l_{int} on I_r is also found to be strongly dependent on the RE seed profile shape, l_{int} increasing with l_{int}^{seed} and, as l_{int} (I_r), the magnetic energy of the RE beam does not scale with I_r^2. The observed peaking also suggests potentially RE MHD unstable plasmas. Integrated modelling of the RE beam formation and termination in ITER has been carried out to investigate current profile shape effects for selected disruption scenarios with Ar and Ne injection using a 1-D disruption model. Low RE generation has been found for the shortest CQs, particularly for the case of Ne, whereas for long CQ times RE currents up to ~10 MA can be produced and, during current termination, the generation of REs by the avalanche mechanism can increase the energy deposited by the REs onto the PFCs up to a few hundreds of MJs (~ $10 \times W_{run}^0$). The peaking of the RE current during the CQ phase decreases with the RE current fraction and the RE beam is found to cross the high-l_{int} empirical stability boundary in l_{int} - q_a space before the expected time for the vertical instability growth (~100 ms). The RE current profile peaking also enhances significantly the role played by the RE avalanche during current termination, increasing the energy conversion efficiency in comparison with 0-D calculations. Mixed Ar+D or Ne+D injection is found to be effective in controlling the formation of the RE current as well as the energy deposited by the REs during current termination. For 7 kPa·m^3 D_2 injection, the magnetic energy converted to kinetic RE energy decreases to $W_{run} \sim 2 \times W_{run}^0$ for the slowest terminations, while 14 kPa·m^3 D injection prevents the conversion of magnetic into RE energy during disruption termination.

Acknowledgements

This work was done under financial support from MINECO (Spain) (Projects No.ENE2012-31753, ENE2015-66444-R), from the ITER Organization under contract IO/13/CT/430000875, carried out within the framework of the EUROfusion Consortium and it has received funding from the Euratom research and training programme 2014-2018 under grant agreement No 633053. ITER is the Nuclear Facility INB no. 174. This paper explores physics processes during the plasma operation of the tokamak when disruptions take place; nevertheless the nuclear operator is not constrained by the results of this paper.The views and opinions expressed herein do not necessarily reflect those of the European Commission or those of the ITER Organization.

References

[1] MARTIN-SOLIS, J.R., et al., *Nucl. Fusion* **54**, 083027 (2014).
[2] MARTIN-SOLIS, J.R., in Fusion Energy 2014 (Proc. 25th Int. Conf., St. Petersburg, 2014) (IAEA) CD-ROM file TH/P3-43.
[3] ERIKSSON, L.-G. et al., *Phys. Rev. Letters* **92**, 205004 (2004).
[4] LOARTE A. et al., *Nucl. Fusion* **51**, 073004 (2011).
[5] MARTIN-SOLIS, J.R., et al., *Phys. Plasmas* **22**, 082503 (2015).
[6] CONNOR, J.W. and HASTIE, R.J., *Nucl.Fusion* **15**, 415 (1975).
[7] ROSENBLUTH, M.N., et al., *Nucl.Fusion* **37**, 1355 (1997).
[8] PUTVINSKI, S., et al., in Fusion Energy 2010 (Proc.23rd Int. Conf., Daejeon, 2010) (Vienna: IAEA) CD-ROM file ITR/1-6.
[9] LUKASH, V.E. et al., Proc. 40th EPS Conf. on Plasma Physics (Helsinki, Finland, 2013) P-5.167.